

Temperature trends at 90 km over Svalbard, Norway (78°N 16°E), seen in one decade of meteor radar observations

C. M. Hall,¹ M. E. Dyrland,² M. Tsutsumi,³ and F. J. Mulligan⁴

Received 17 October 2011; revised 15 March 2012; accepted 16 March 2012; published 20 April 2012.

[1] Temperatures at 90 km altitude above Svalbard (78°N, 16°E) have been determined using a meteor wind radar and subsequently calibrated by satellite measurements for the period autumn 2001 to present. The dependence of the temperatures on solar driving has been investigated using the Ottawa 10.7 cm flux as a proxy. Removing the response of the temperatures to the seasonal and solar cycle variations yields a residual time series which exhibits the negative trend of -4 ± 2 K decade⁻¹. We indicate that, given the month-to-month variability and memory in the time series, for a 90% confidence in this trend, we require only 55 months of data – considerably less than the amount available. Cooling of the middle atmosphere, which would be strongly supported by these results, would result in contraction and subsequent lowering of pressure surfaces; we explain that including a negative trend in the pressure model used to obtain temperatures from meteor train echo fading times would also merely serve to augment the observed 90 km cooling.

Citation: Hall, C. M., M. E. Dyrland, M. Tsutsumi, and F. J. Mulligan (2012), Temperature trends at 90 km over Svalbard, Norway (78°N 16°E), seen in one decade of meteor radar observations, *J. Geophys. Res.*, 117, D08104, doi:10.1029/2011JD017028.

1. Introduction

[2] The increase of atmospheric concentration of carbon dioxide (CO₂), methane and other so-called greenhouse gases during the last century has led to a heating of the troposphere. These greenhouse gases are also expected to modify the mesosphere, thermosphere and ionosphere: for the middle atmosphere, theories and models predict a cooling to occur as a result of increased infrared thermal emissions by CO₂ [e.g., Roble and Dickinson, 1989; Akmaev and Formichev, 1998]. The polar mesopause region (80–100 km) has been highlighted as a place where one can expect to see the largest changes, and especially for the summer season where the occurrences of polar mesospheric clouds (PMC) and polar mesospheric summer echoes (PMSE) are closely connected to the temperature [Thomas, 1996]. In a review paper on long-term changes and trends in mesopause region temperatures, Beig *et al.* [2003] summarize that while some authors have reported negative trends, many authors have found no significant cooling during the last couple of decades. This lack of significant temperature trends near the mesopause has also been reproduced in recently developed atmospheric climate models [e.g., Schmidt *et al.*, 2006], in which seasonal differences in the response of mesopause

region temperatures to an increase of CO₂ have also been noted. They show that a cooling trend is expected to be enhanced during the summer and reduced during the winter, due to changes in the large-scale circulation connected to the temperature change. Even more recently, Beig [2011] revises the overview of the previous paper; to quote: “some of the new results now indicate a break in trend and tendency of negative signal where earlier no trend feature was noticed.” The conflicting reports on this matter are part of the main motivation for continuing to study these temperature series and look for trends.

[3] The Svalbard archipelago is an excellent location for the studies of mesopause region temperatures and dynamics. Its main township Longyearbyen is located at a high arctic latitude (78°N, 16°E), but nevertheless has a well-developed infrastructure and is easily accessible by regular aircraft services. One of the instruments deployed there is the Nippon/Norway Svalbard Meteor Radar (NSMR). Located in Adventdalen only 10 km from Longyearbyen, it has measured mesopause region temperatures and winds since 2001. Reports on this temperature series have been given by Hall *et al.* [2004, 2006], but it is not until now that the time series has become long enough for a trend analysis to be viable. In this paper we report trends observed in temperatures measured by the NSMR meteor radar between October 2001 and October 2011 (~10 years). A new calibration routine for the meteor temperatures is also used, in which measurements of temperature from the Microwave Limb Sounder on the Aura satellite [Schwartz *et al.*, 2008] replace the ground-based optical measurements of rotational hydroxyl temperatures and lidar temperatures used previously [Dyrland *et al.*, 2010]. The quantitative confidence in the results of the trend analysis are given, and finally the

¹Tromsø Geophysical Observatory, University of Tromsø, Tromsø, Norway.

²University Centre in Svalbard, Longyearbyen, Norway.

³National Institute of Polar Research, Tokyo, Japan.

⁴Department of Experimental Physics, National University of Ireland, Maynooth, Ireland.

results are discussed in relation to earlier studies of mesopause region trends.

2. Meteor Wind Radar Measurements and Analysis

[4] The particular method used for derivation of neutral temperatures from meteor trail echoes has been fully described by *Dyrland et al.* [2010], however we shall provide a précis here. By observing ionization trails from meteors using a radar operating at a frequency less than the plasma frequency of the electron density in the trail (the so-called “underdense” condition), it is possible to derive ambipolar diffusion coefficients D from the radar echo decay times τ according to:

$$\tau = \frac{\lambda^2}{16\pi^2 D} \quad (1)$$

wherein λ is the radar wavelength. Thereafter the temperature T may be derived using the relation:

$$T = \sqrt{\frac{P \cdot D}{6.39 \times 10^{-2} K_0}} \quad (2)$$

where P is the pressure and K_0 is the zero field mobility of the ions in the trail (here we assume $K_0 = 2.4 \times 10^{-4} \text{ m}^{-2} \text{ s}^{-1} \text{ V}^{-1}$). Explanations of the theories and assumptions of the complete method for determining neutral air temperatures from meteor trail echoes have been discussed exhaustively earlier, for example: *McKinley* [1961], *Chilson et al.* [1996], *Cervera and Reid* [2000] and *Holdsworth et al.* [2006]. Important work has also been done by *Hocking* in order to achieve independence from use of pressure models [e.g., *Hocking*, 2011, and references therein]; however pressure gradients are still required as input. As explained forthwith, however, we circumvent the pressure model problems and will not enter into an evaluation of various approaches to temperature derivation here.

[5] In this study, we obtain the necessary echo fading times from the Nippon/Norway Svalbard Meteor Radar (NSMR) described in detail elsewhere [*Hall et al.*, 2006]. The radar is located at 78.33°N, 16.00°E in Adventdalen and operates at 31 MHz fully automated with a height resolution of 1 km. The radar came into operation in the spring of 2001, but due to system changes during the first months of operation we shall only use data from October 2001 onwards. At 31 MHz the maximum echo occurrence rate is at 90 km altitude; we shall concentrate on this altitude in this study, avoiding height regimes above and below in which there are steep gradients in occurrence rate within the meteor echo region. For NSMR, a typical daily rate might be 2000 detections with a distribution, centered on 90 km altitude, of width 10 km at half of peak value, and with approximately 40–100 echoes per hour. Although it is possible to examine temperature variations with a 30 min resolution (due to the large number of echoes and less pronounced diurnal variation relative to midlatitude systems), we shall work with daily mean values. For NSMR the intraday variation in echo rates is not as pronounced as for lower latitude stations and we do not expect a tidally induced bias induced by particularly high echo rates at specific tidal phases.

The pressure model used here is that of *Lübken and von Zahn* [1991] combined with that of *Lübken* [1999], and it is the same as was used by *Holdsworth et al.* [2006], *Hall et al.* [2006] and *Dyrland et al.* [2010]. In the *Hall et al.* [2006] paper the initial daily mean temperature estimates for 78°N were too high to be real, believed to result, in part, from the pressure model not being appropriate for such a high latitude. In fact, *Manson et al.* [2011a] demonstrate the zonal differences (specifically between Eureka at 86°W and Svalbard at 16°E). The initial temperature estimates were therefore adjusted/calibrated using OH emission derived temperatures (from winter months) and potassium lidar measurements (from the summer months). For this study we chose the same initial approach, but calibrated by comparison with temperatures measured by the instrument MLS (Microwave Limb Sounder) on board NASA’s EOS (Earth Observing System) Aura satellite instead of the ground-based measurements from Longyearbyen [*Dyrland et al.*, 2010]. This choice is founded on work by *Mulligan et al.* [2009], who found that the OH emission peak altitude above Longyearbyen can vary between 75 and 90 km. Since the calibration of meteor radar temperatures from *Hall et al.* [2006] were based on the assumption that the OH layer peak height was at the nominal ~86 km and thus extrapolated them from there to 90 km according to the model [*Lübken and von Zahn*, 1991; *Lübken*, 1999] gradients, this assumption likely introduced a large variability in the temperature set that did not necessarily reflect real variations of the temperature at 90 km. The amount of data available for calibration was also limited, as the potassium lidar was only operational at Longyearbyen during the summer seasons 2001–2003. Daily averages of OH temperatures were only available in the period from mid November to late February, and the number varied strongly from season to season. The high number of temperatures measured during the anomalously warm 2003–2004 season [*Dyrland and Sigernes*, 2007], might therefore lead to a biased temperature set. Since MLS data are available for the full year since August 2004, we use them for the calibration instead, as explained by *Dyrland et al.* [2010]. At the altitudes of the radar temperature retrievals, 90 km, the vertical resolution of the Aura MLS temperatures is 13 K with a precision of 3 K [*Schwartz et al.* 2008]. Despite the apparently low altitude resolution, these temperatures proved very valuable and were found to be particularly stable over several years in a recent comparison of satellite temperatures with ground-based optical measurements made at Davis Station, Antarctica [*French and Mulligan*, 2010]. Thus, in Figure 1 we show resulting “first estimate” temperatures together with the corresponding Aura MLS measurements. The result of the calibration described above is shown in Figure 2 (which also includes the Aura MLS values), and they are these data we shall employ in the trend analysis which follows. Since Aura MLS temperatures are retrieved on a fixed pressure grid, we repeated the trend analysis using Aura temperatures at a fixed pressure level of 0.001 hPa corresponding to approximately 90 km altitude, and found no significant difference in the results.

3. Trend Analysis

[6] The data shown in Figure 2 exhibit considerable day-to-day fluctuations due to gravity and planetary wave modulation,

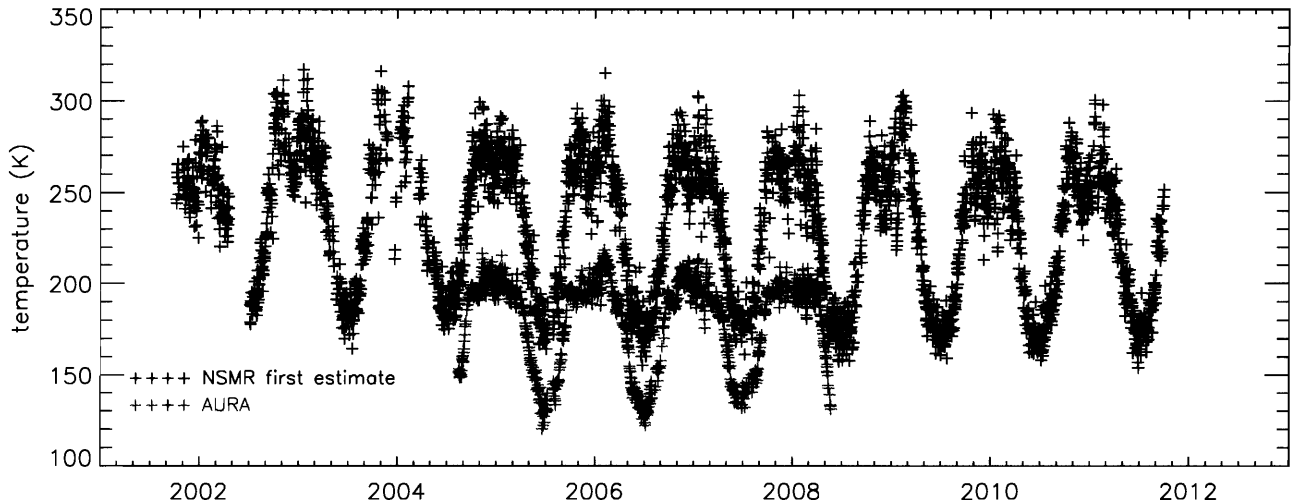


Figure 1. First estimates of 90 km temperatures using meteor radar data together with those measured by the MLS instrument on the Aura satellite.

interesting in their own right. However, here we investigate the trends already discernible, albeit qualitatively, in Figure 2. Problems with the radar prior to July 2002 render these data suspect and we exclude them herewith. We shall not discriminate between summer and winter periods in this initial study. First we shall separate the seasonal variation. A monthly climatology is determined by averaging all January, February, etc., values, resulting in Figure 3. The seasonal variation is as to be expected with a summer minimum with a temperature of around 135 K. Larger standard deviations in winter reflect the larger planetary wave activity compared to summer. Next, these monthly values are subtracted from the original (calibrated) data to arrive at residuals exhibiting no seasonal variation. Spectral and probability density function analyses, not shown here, have confirmed this. These simple findings (Figure 4) are misleading though, because the middle atmosphere can be

expected to respond to heating due to absorption of solar UV radiation by ozone and the former varies through a solar cycle. Quite apart from increased heating of the underlying stratosphere during solar maximum, the ozone profile exhibits a secondary maximum [e.g., *Evans and Llewellyn, 1972*] near to the peak occurrence height for meteor echoes, 90 km in this case, so we can anticipate local temperature variation controlled by the UV flux. In order to investigate this, we have performed a simple linear regression of the 30-point Lee-filtered [*Lee, 1986*] daily residual temperatures on the corresponding $f_{10.7}$ fluxes, as shown in Figure 5. As is evident from the scatterplots in Figure 5, the reliability of the regression line is considerably enhanced by using the filtered values, this filtering corresponding to a 1-month low-pass filter. The temperatures increase with increasing UV flux as expected: $+0.16 \text{ K flux-unit}^{-1} \pm 2\%$ (flux-units are $\text{Wm}^{-2}\text{Hz}^{-1}$).

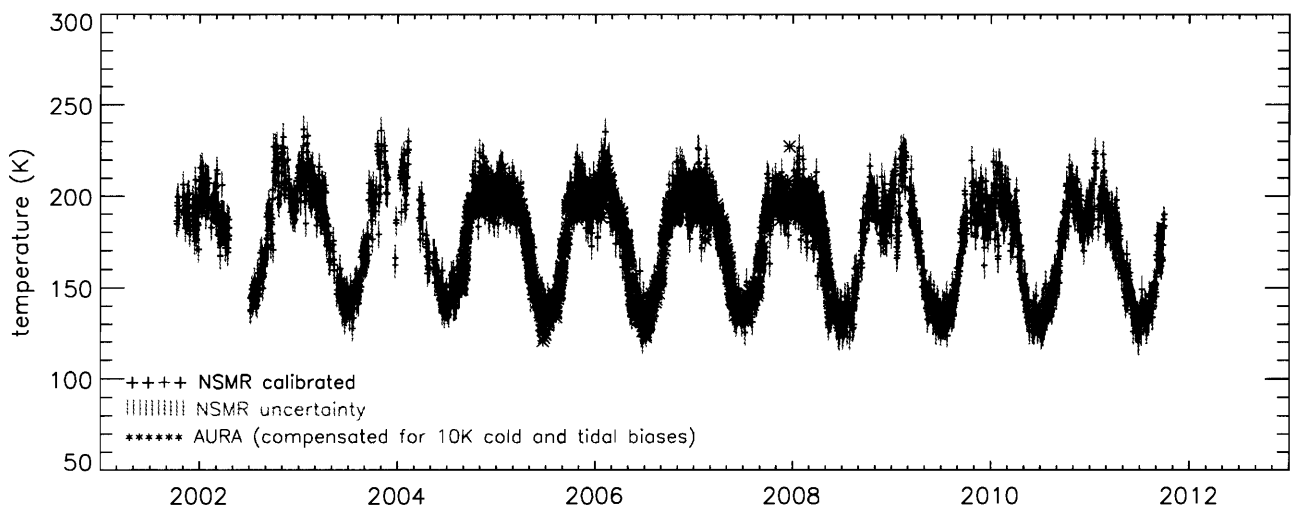


Figure 2. Daily mean temperatures derived from NSMR at 90 km altitude using calibration by Aura MLS as described in the text. Earlier data were subject to changes in radar configuration and are excluded, although the entire lifetime of the radar extends from Spring 2001.

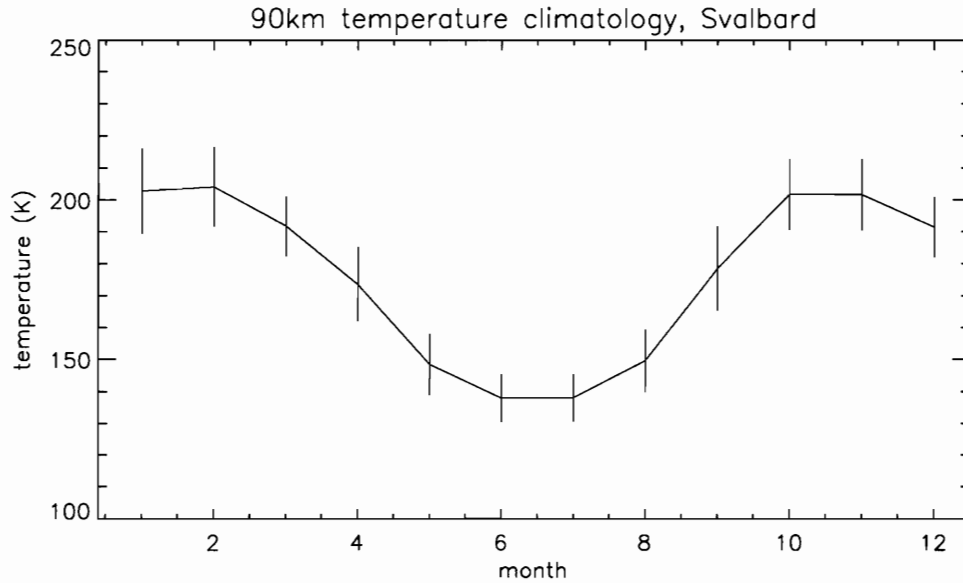


Figure 3. Monthly climatology obtained by averaging all January, February, etc., values. Vertical bars indicate standard deviations.

[7] Accepting the simple dependencies in Figure 5, then, a solar-driven temperature series is derived from the $f_{10.7}$ flux, and subtracted from the original series to give residual temperatures, T' :

$$T' = T - (a + b \cdot f_{10.7}) \quad (3)$$

where a and b are the coefficients of the linear regression. The method is much the same as that used by, for example *Ulich and Turunen* [1997] and more recently *Hall et al.* [2007] to remove the effects of solar radiation from ionospheric time series. The final result is shown in Figure 6. In order to eliminate short-term deterministic signals (e.g., multiday period waves) and to prepare for a trend analysis, monthly means are then calculated, through which we fit a

linear trend, as shown in Figure 7. The monthly mean residuals (viz. temperatures after removal of seasonal variation and solar influence), therefore exhibit a negative trend of $4 \pm 2 \text{ K decade}^{-1}$. Included in Figure 7 are the 95% confidence limits in the linear fit [*Working and Hotelling, 1929*].

4. Confidence and Significance

[8] Let us now address the significance of the above finding and our confidence in it. From *Tiao et al.* [1990] we see that a trend is considered to be significantly non-zero at the 5% level if its absolute value is greater than the 2σ uncertainty in slope assuming a normal distribution. *Weatherhead et al.* [2002] have subsequently built upon work by *Weatherhead et al.* [1998] and *Tiao et al.* [1990]

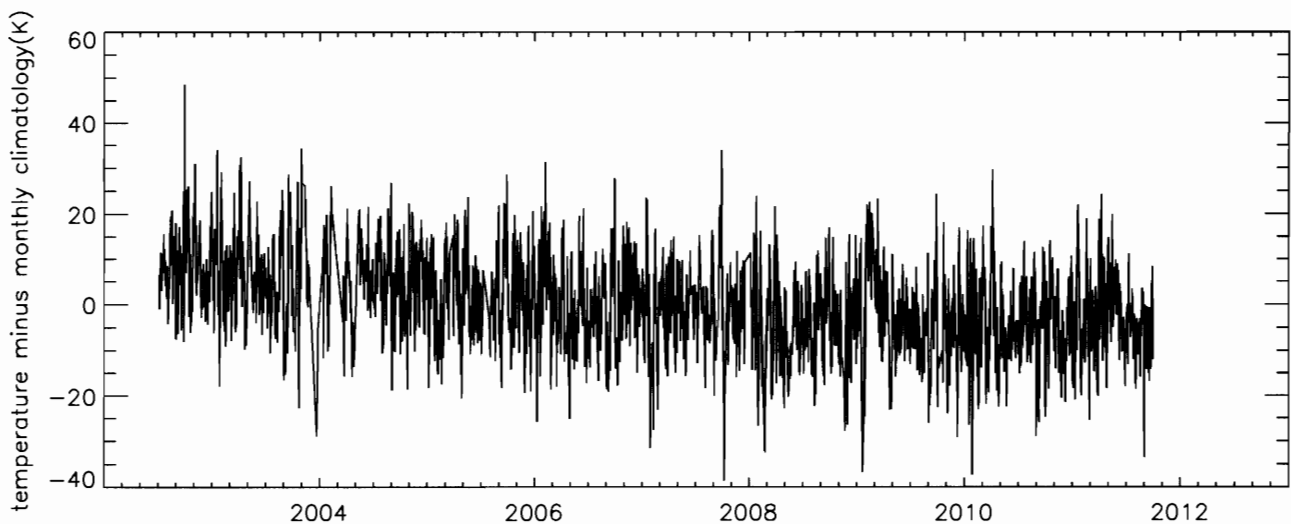


Figure 4. Daily (residual) temperatures obtained by subtracting the monthly climatology from the calibrated temperature series.

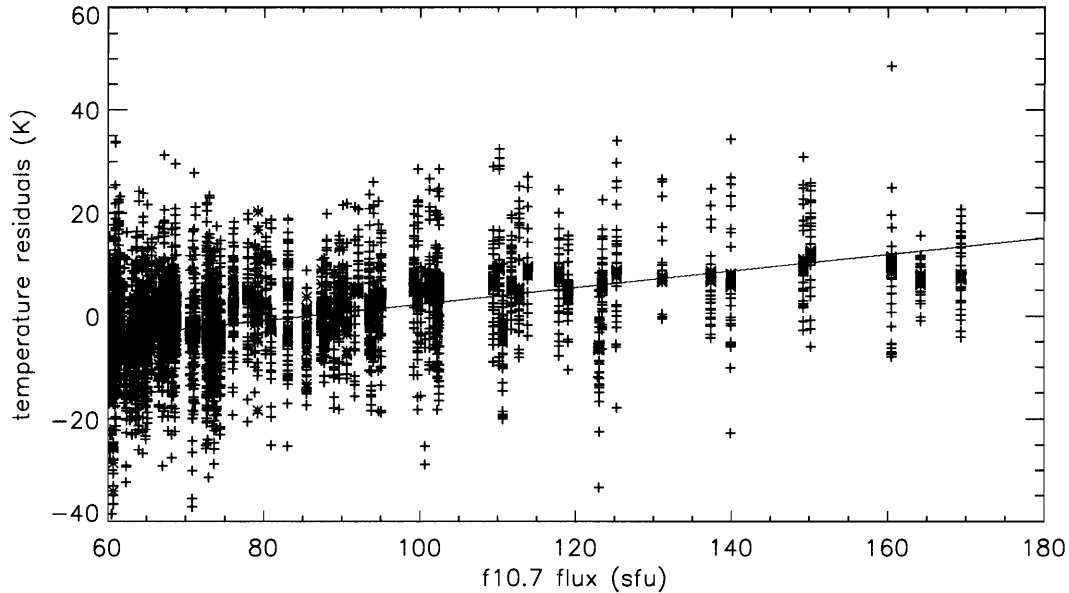


Figure 5. Scatterplot of the daily residual temperatures versus the corresponding f10.7 fluxes (pluses). Linear regression is performed using 30-point (i.e., 1-month) Lee-filtered daily residual temperatures (asterisks) on the corresponding f10.7 fluxes.

and define a minimum time series length n^* for which a trend can be considered detectable:

$$n^* \cong \left[\frac{j\sigma_N}{|\omega_0|} \sqrt{\frac{1+\phi}{1-\phi}} \right]^{2/3} \quad (4)$$

where σ_N is the month-to-month variability in the data as we determined earlier, ω_0 is the expected trend, ϕ is the autocorrelation in the month-to-month data (i.e., the autocorrelation at lag 1). *Tiao et al.* [1990] and *Weatherhead et al.* [2002] use $j = 3.3$ for 90% probability that a trend ω_0 is detectable after n^* (ω_0 and n^* having the same time units)

assuming a Gaussian distribution (and also a data set with noise characterized as an autoregressive – AR(1) - process). *Hall et al.* [2011], working with ionospheric E region height and critical frequency time series critically investigated the very distributions, finding the stochastic component of the critical frequency data set (for example) to be better characterized as fractional Gaussian noise. Also, *Rypdal and Rypdal* [2010] have similarly established that solar forcing is probably non Gaussian. However, the length of the time series we present in this study does not lend itself (yet) to a reliable investigation of the stochastic component in terms of complexity and for the time being we assume the noise to be a Gaussian process and the time series to

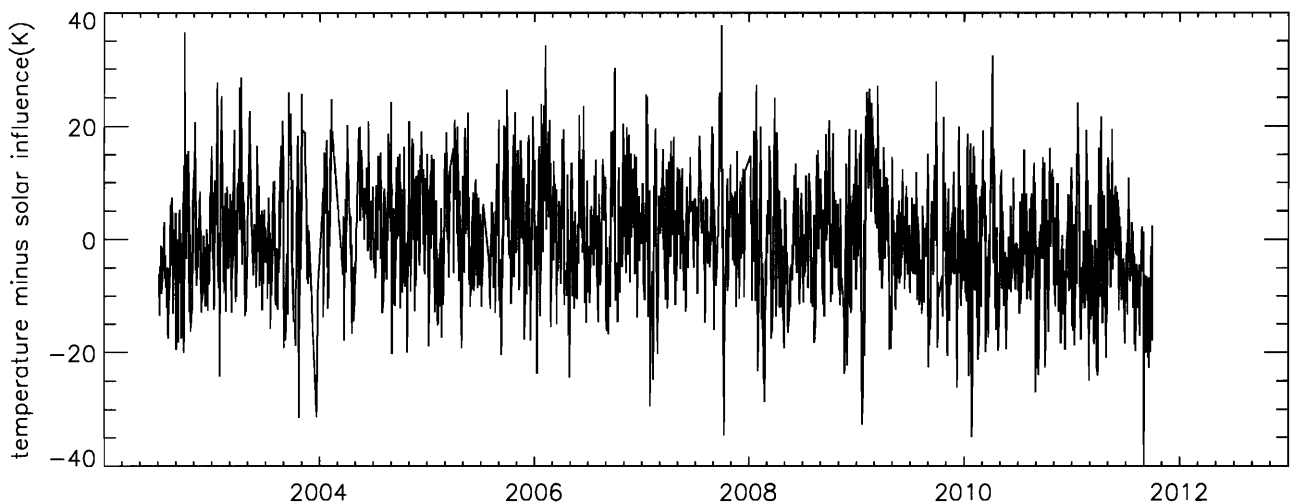


Figure 6. Temperature residuals after removal of both seasonal (i.e., expressed as monthly climatology) variation and solar UV flux effects. This residual now comprises the stochastic component of the signal and with any trend imposed upon it.

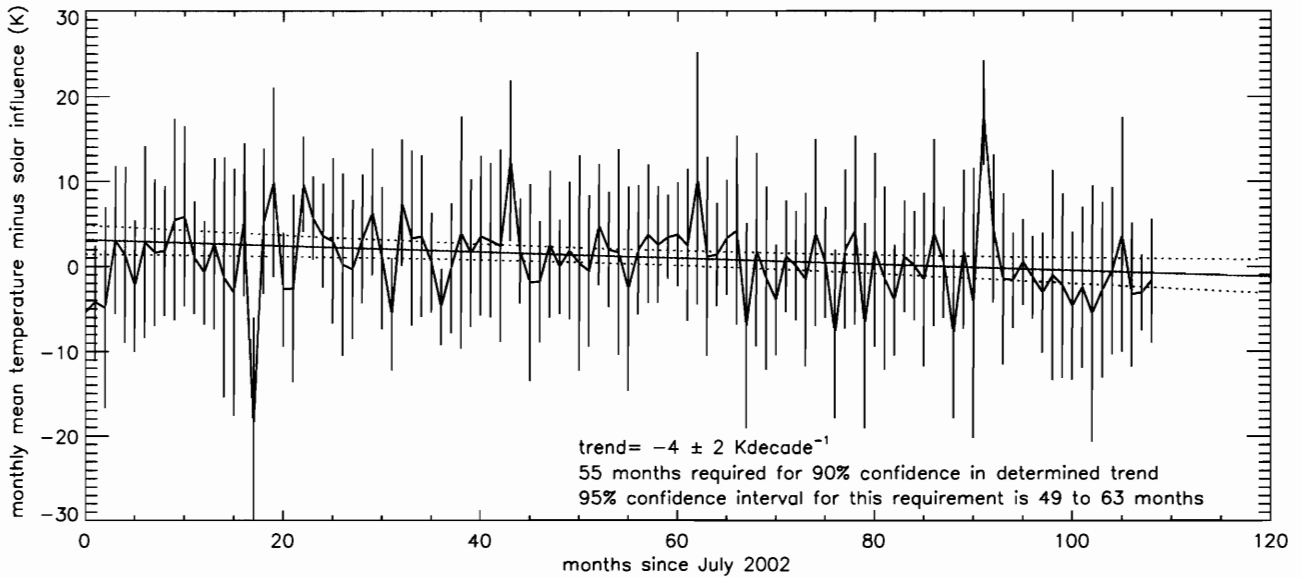


Figure 7. Monthly means (thick line) of residual temperatures (seasonal variation and solar-cycle effects removed) together with respective standard deviations (vertical bars). The linear fitted trend (straight line) is superimposed together with its 95% confidence limits (dotted hyperbolae). See text for explanation of annotation.

be autoregressive. Following *Tiao et al.* [1990], the trend of -4 K decade^{-1} is therefore just significant at the 5% level with an uncertainty ($1-\sigma$) in slope of 2 K decade^{-1} . Furthermore, equation (4) reveals that the minimum time series length for the -4 K decade^{-1} trend is 55 months – approximately half the available length to date, namely, 109 months taking into account exclusion of data prior to July 2002. Additionally, *Weatherhead et al.* [1998] also indicate a means of determining the 95% confidence interval for n^* :

$$\left\{ n^* e^{\pm \frac{4}{3\sqrt{M}} \sqrt{\frac{1+\psi}{1-\psi}}} \right\} \quad (5)$$

where M is the number of months of data (which at the time of writing equals 109). From this we find the 95% confidence interval in n^* (which currently equals 55 months) to be [49,63] months. We may be allowed, therefore, considerable sureness in our trend determination. In fact, *Hall et al.* [2011] found that the true probability density function of the analogous stochastic component for E region critical frequency implied shorter n^* than if a Gaussian was assumed.

5. Physical Processes

[9] The mechanism proposed for cooling is that gases causing the increasing greenhouse effect in the troposphere act as refrigerants in the middle atmosphere [Roble and Dickinson, 1989; Rishbeth, 1990]. A general cooling of the middle atmosphere would cause a shrinking and a general lowering of pressure surfaces. Since the pressure model we use here (in equation (2)) only varies with season, we must address the effects of a climatic change in pressure at 90 km. In equation (2) we see that temperature depends on the square roots of both diffusivity and pressure such that if both entities are subject to negative trends, the negative trend in

temperature will only increase. Although a simplistic scenario, it serves to demonstrate that a trend in pressure commensurable with middle atmosphere cooling and the accepted mechanism for the secular decrease in E region altitude [e.g., *Hall et al.*, 2007, 2011] will not cancel out the trend in diffusivity when converting to temperature, but, rather, augment it. It should be noted that we have assumed that the calibration to the AURA measurements is constant over the 10 year period, and furthermore the spatial averaging of the AURA data is also larger than that of the radar and results can be affected by data from, for example, outside the polar vortex [*Manson et al.*, 2011a].

[10] We have so far restricted our study to 90 km altitude, that of the peak in echo occurrence for NSMR, operating at 31 MHz. Immediately above and below this height the number of echoes decays considerably within one (1 km) range gate such that the diffusivities we obtain may not be representative for that height. However, a potentially more serious problem is that a few km above the peak height, electrodynamics begins to influence the diffusion of the meteor trail as discussed by *Dyrud et al.* [2001]. Below around 80 km, the derived diffusivity becomes almost independent of altitude suggesting either limitations of the radar or as discussed by *Hall et al.* [2005] and *Ballinger et al.* [2008], additional atmospheric processes. The issue addressed by *Ballinger et al.* [2008] applies to the weak population of echoes, but at all heights in the regime via a reduction in observed decay time (and therefore increase in derived diffusivity) can arise from, for example, electron-ion recombination and also scavenging of free electrons by aerosols and macro ions [e.g., *Havnes and Sigernes*, 2005]. Applying such a scenario here would imply an overestimation of diffusivity leading to an overestimation of temperature, such that correcting for these effects would give rise to lower temperatures than reported here. Recombination processes in general depend weakly and inversely on electron

temperature and on particle number densities (both charged and, depending on the nature of the recombination process, neutral) [e.g., Brekke, 1997], but how recombination rates, particularly near the mesopause, may vary climatically is a problem outside the scope of this study. At a fixed altitude and given temperature, a reduction in pressure would lead to a reduction in neutral number density and therefore a decrease in average electron density in meteor trails - i.e., a trend toward weaker echoes. From Ballinger *et al.* [2008], who address the region 80–90 km in particular, this could lead to underestimation of temperature.

[11] Given the pitfalls in temperature estimation above [Dyrud *et al.*, 2001] and below [Ballinger *et al.*, 2008] 90 km, we feel that our “safe” approach of “sticking to” 90 km is justified. It is unfortunate we find this necessary, because 90 km is the assumed altitude of the summer mesopause at 78°N [Höffner and Lübken, 2007] (although see the modeling results reported by Manson *et al.* [2011a, 2011b]) and by examining altitudes between 80 and 100 km with NSMR one could search for trends both above and below the summer mesopause, and for that matter in a 20 km deep regime of the winter mesosphere.

[12] Unfortunately, there are few studies available with which to compare our results. Analyses of the previously mentioned OH(6–2) rotational temperature series from Svalbard measured in winters 1983–2005 have failed to reveal any statistically significant trend [Sigernes *et al.*, 2003; Dyrland and Sigernes, 2007]. The non-statistically significant trends reported in these studies were of the order of +2 K decade⁻¹, i.e., of the opposite sign compared to our findings. However, for these assessments solar forcing was not accounted for as no solar cycle dependency was found in the series [Sigernes *et al.*, 2003]. Also, monthly averages containing sudden stratospheric warming events were excluded from the analysis. This and recent knowledge about the highly varying OH emission height above Longyearbyen [Mulligan *et al.*, 2009], would complicate the comparison with the observed 90 km trend. Blum and Fricke [2008] have investigated temperature differences between in situ (falling sphere) measurements primarily from the interval 1989–1993 and lidar measurements primarily from 2002 to 2006 - i.e., over approximately one decade, for 69°N at 16°E. In the height regime 65–70 km (the highest in their study), they report a temperature decrease of 7 K, which, considering altitude and geographic differences, and not least uncertainties in such estimates in general, is not dissimilar to our findings. One of the very latest updates on temperature trend determinations is that of Beig [2011]. The reader is referred to this review to further investigate the references therein which are too numerous to reproduce here. An essential finding is that more evidence of mesopause region cooling has come to light in recent years, e.g., subsequent to the time series analyzed by Sigernes *et al.* [2003] obtained by optical measurements from the same location as NSMR. Moreover, the trends identified in a number of studies reported by Beig [2011] suggest values ranging from 1 or 2 K decade⁻¹ to as much as 7 K decade⁻¹. Another high latitude feature not sufficiently understood is the stability and strength of the two polar vortices (20 to 80–100 km), upon which the other near-pole’s temperatures depend. The Scandinavia- Svalbard location is most often the preferred site of the winter-polar vortex making the observations reported here atypical for

~80°N. Thus it might be more appropriate to think in terms of temperature change “during the last decade” rather than “per decade” and specifically for Svalbard. With the limited data set used in this study, however we are unable to pursue this further.

6. Conclusions

[13] Using the Nippon/Norway Svalbard Meteor Radar, we have determined echo fading times from meteor trails and subsequently ambipolar diffusion coefficients and finally daily average temperature estimates. The temperatures have then been calibrated using Aura MLS data. Taking the data set from October 2001 to present, we identify a fall in neutral atmosphere temperature at 90 km altitude, 78°N, 16°E that is independent of solar forcing and could therefore be interpreted as anthropogenic (although we refrain from exploring this hypothesis in this study). We further explain that a climatic decrease in pressure will only lead to these trends being underestimated. For 90 km we find a change of approximately -4 ± 2 K decade⁻¹ after removal of solar cycle and seasonal variation. For 90% confidence in this value, given the variability and memory in the time series, we would require only 55 months of data (the 95% confidence interval in this being 49–63 months). Our conclusion therefore is that there is indeed a cooling of the neutral atmosphere at 90 km above Svalbard in the Norwegian high Arctic, amounting to 4 ± 2 K during the last decade.

[14] **Acknowledgments.** The authors wish to acknowledge Takahiko Aso for his initiative in establishing a meteor radar on Svalbard. We thank the Aura/MLS science team for providing data used in this study. Thanks go to the reviewers of this manuscript.

References

- Akmaev, R. A., and V. I. Formichev (1998), Cooling of the mesosphere and lower thermosphere due to doubling of CO₂, *Ann. Geophys.*, *16*, 1501–1512.
- Ballinger, A. P., P. B. Chilson, R. D. Palmer, and N. J. Mitchell (2008), On the validity of the ambipolar diffusion assumption in the polar mesopause region, *Ann. Geophys.*, *26*, 3439–3443, doi:10.5194/angeo-26-3439-2008.
- Beig, G. (2011), Long-term trends in the temperature of the MLT region: 1. Anthropogenic, *J. Geophys. Res.*, *116*, A00H11, doi:10.1029/2011JA016646.
- Beig, G., et al. (2003), Review of mesospheric temperature trends, *Rev. Geophys.*, *41*(4), 1015, doi:10.1029/2002RG000121.
- Blum, U., and K. H. Fricke (2008), Indications for a long-term temperature change in the polar summer middle atmosphere, *J. Atmos. Sol. Terr. Phys.*, *70*, 123–137, doi:10.1016/j.jastp.2007.09.015.
- Brekke, A. (1997), *Physics of the Upper Polar Atmosphere*, 491 pp., John Wiley, Chichester, U. K.
- Cervera, M. A., and I. M. Reid (2000), Comparison of atmospheric parameters derived from meteor observations with CIRA, *Radio Sci.*, *35*, 833–843, doi:10.1029/1999RS002226.
- Chilson, P. B., P. Czechowsky, and G. Schmidt (1996), A comparison of ambipolar diffusion coefficients in meteor trains using VHF radar and UV lidar, *Geophys. Res. Lett.*, *23*, 2745–2748, doi:10.1029/96GL02577.
- Dyrland, M. E., and F. Sigernes (2007), An update on the hydroxyl airglow temperature record from the Auroral Station in Adventdalen, Svalbard (1980–2005), *Can. J. Phys.*, *85*(2), 143–151, doi:10.1139/P07-040.
- Dyrland, M. E., C. M. Hall, F. J. Mulligan, and M. Tsutsumi (2010), Improved estimates for neutral air temperatures at 90 km and 78°N using satellite and meteor radar data, *Radio Sci.*, *45*, RS4006, doi:10.1029/2009RS004344.
- Dyrud, L. P., M. M. Oppenheim, and A. F. vom Endt (2001), The anomalous diffusion of meteor trails, *Geophys. Res. Lett.*, *28*, 2775–2778, doi:10.1029/2000GL012749.
- Evans, W. F. J., and E. J. Llewellyn (1972), Measurements of mesospheric ozone from observations of the 1.27 μ band, *Radio Sci.*, *7*, 45–50, doi:10.1029/RS007i001p00045.

- French, W. J. R., and F. J. Mulligan (2010), Stability of temperatures from TIMED/SABER v1.07(2002–2009) and Aura/MLS v2.2(2004–2009) compared with OH(6–2) temperatures observed at Davis Station, Antarctica, *Atmos. Chem. Phys.*, *10*, 11,439–11,446, doi:10.5194/acp-10-11439-2010.
- Hall, C. M., T. Aso, M. Tsutsumi, J. Höffner, and F. Sigernes (2004), Multi-instrument derivation of 90 km temperatures over Svalbard (78°N 16°E), *Radio Sci.*, *39*, RS6001, doi:10.1029/2004RS003069.
- Hall, C. M., T. Aso, M. Tsutsumi, S. Nozawa, A. H. Manson, and C. E. Meek (2005), Testing the hypothesis of the influence of neutral turbulence on deduction of ambipolar diffusivities from meteor trail expansion, *Ann. Geophys.*, *23*, 1071–1073, doi:10.5194/angeo-23-1071-2005.
- Hall, C. M., T. Aso, M. Tsutsumi, J. Höffner, F. Sigernes, and D. A. Holdsworth (2006), Neutral air temperatures at 90 km and 70° and 78°N, *J. Geophys. Res.*, *111*, D14105, doi:10.1029/2005JD006794.
- Hall, C. M., A. Brekke, and P. S. Cannon (2007), Climatic trends in E region critical frequency and virtual height above Tromsø (70°N, 10°E), *Ann. Geogr.*, *25*, 2351–2357.
- Hall, C. M., K. Rypdal, and M. Rypdal (2011), The E region at 69°N 19°E: Trends, significances and detectability, *J. Geophys. Res.*, *116*, A05309, doi:10.1029/2011JA016431.
- Havnes, O., and F. Sigernes (2005), On the influence of background dust on radar scattering from meteor trails, *J. Atmos. Sol. Terr. Phys.*, *67*, 659–664, doi:10.1016/j.jastp.2004.12.009.
- Hocking, W. K. (2011), A review of Mesosphere-Stratosphere-Troposphere (MST) radar developments and studies, circa 1997–2008, *J. Atmos. Sol. Terr. Phys.*, *73*, 848–882, doi:10.1016/j.jastp.2010.12.009.
- Höffner, J., and F.-J. Lübken (2007), Potassium lidar temperatures and densities in the mesopause region at Spitsbergen (78°N), *J. Geophys. Res.*, *112*, D20114, doi:10.1029/2007JD008612.
- Holdsworth, D. A., R. J. Morris, D. J. Murphy, I. M. Reid, G. B. Burns, and W. J. R. French (2006), Antarctic mesospheric temperature estimation using the Davis MST radar, *J. Geophys. Res.*, *111*, D05108, doi:10.1029/2005JD006589.
- Lee, J. S. (1986), Speckle suppression and analysis for synthetic aperture radar images, *Opt. Eng.*, *25*, 636–643.
- Lübken, F.-J. (1999), Thermal structure of the Arctic summer mesosphere, *J. Geophys. Res.*, *104*, 9135–9149.
- Lübken, F.-J., and U. von Zahn (1991), Thermal structure of the mesopause region at polar latitudes, *J. Geophys. Res.*, *96*, 20,841–20,857, doi:10.1029/91JD02018.
- Manson, A. H., C. E. Meek, X. Xu, T. Aso, J. R. Drummond, C. M. Hall, W. K. Hocking, M. Tsutsumi, and W. E. Ward, (2011a) Characteristics of Arctic winds at CANDAC-PEARL (80°N, 86°W) and Svalbard (78°N, 16°E) for 2006–2009: Radar observations and comparisons with the model CMAM-DAS, *Ann. Geophys.*, *29*, 1927–1938.
- Manson, A. H., C. E. Meek, X. Xu, T. Aso, J. R. Drummond, C. M. Hall, W. K. Hocking, M. Tsutsumi, and W. E. Ward, (2011b) Characteristics of Arctic tides at CANDAC-PEARL (80°N, 86°W) and Svalbard (78°N, 16°E) for 2006–2009: Radar observations and comparisons with the model CMAM-DAS, *Ann. Geophys.*, *29*, 1939–1954.
- McKinley, D. W. R. (1961), *Meteor Science and Engineering*, 309 pp., McGraw-Hill, New York.
- Mulligan, F. J., M. E. Dyrlund, F. Sigernes, and C. S. Deehr (2009), Inferring hydroxyl layer peak heights from ground-based measurements of OH(6–2) band radiance at Longyearbyen (78°N, 16°E), *Ann. Geophys.*, *27*, 4197–4205.
- Rishbeth, H. (1990), A greenhouse effect in the ionosphere?, *Planet. Space Sci.*, *38*, 945–948.
- Roble, R. G., and R. E. Dickinson (1989), How will changes in carbon dioxide and methane modify the mean structure of the mesosphere and thermosphere?, *Geophys. Res. Lett.*, *16*, 1441–1444, doi:10.1029/GL016i012p01441.
- Rypdal, M., and K. Rypdal (2010), Testing the hypothesis about sun-climate complexity linking, *Phys. Rev. Lett.*, *104*, 128501, doi:10.1103/PhysRevLett.104.128501.
- Schmidt, H., et al. (2006), The HAMMONIA chemistry climate model: Sensitivity of the mesopause region to the 11-year solar cycle and CO₂ doubling, *J. Clim.*, *19*, 3903–3931, doi:10.1175/JCLI3829.1.
- Schwartz, M. J., et al. (2008), Validation of the Aura Microwave Limb Sounder temperature and geopotential height measurements, *J. Geophys. Res.*, *113*, D15S11, doi:10.1029/2007JD008783.
- Sigernes, F., N. Shumilov, C. S. Deehr, K. P. Nielsen, T. Svenøe, and O. Havnes (2003), The Hydroxyl rotational temperature record from the Auroral Station in Adventdalen, Svalbard (78°N, 15°E), *J. Geophys. Res.*, *108*(A9), 1342, doi:10.1029/2001JA009023.
- Thomas, G. E. (1996), Is the polar mesosphere the miner's canary of global change?, *Adv. Space Res.*, *18*, 149–158, doi:10.1016/0273-1177(95)00855-9.
- Tiao, G. C., G. C. Reinsel, D. Xu, J. H. Pedrick, X. Zhu, A. J. Miller, J. J. DeLuisi, C. L. Mateer, and D. J. Wuebbles (1990), Effects of autocorrelation and temporal sampling schemes on estimates of trend and spatial correlation, *J. Geophys. Res.*, *95*(D12), 20,507–20,517, doi:10.1029/JD095iD12p20507.
- Ulich, T., and E. Turunen (1997), Evidence for long-term cooling of the upper atmosphere in ionosonde data, *Geophys. Res. Lett.*, *24*, 1103–1106, doi:10.1029/97GL50896.
- Weatherhead, E. C., et al. (1998), Factors affecting the detection of trends: Statistical considerations and applications to environmental data, *J. Geophys. Res.*, *103*(D14), 17,149–17,161, doi:10.1029/98JD00995.
- Weatherhead, E. C., A. J. Stevermer, and B. E. Schwartz (2002), Detecting environmental changes and trends, *Phys. Chem. Earth*, *27*, 399–403.
- Working, H., and H. Hotelling (1929), Application of the theory of error to the interpretation of trends, *J. Am. Stat. Assoc.*, *24*, 73–85, doi:10.2307/2277011.

M. E. Dyrlund, University Centre in Svalbard, N-9171 Longyearbyen, Norway.

C. M. Hall, Tromsø Geophysical Observatory, University of Tromsø, N-9037 Tromsø, Norway. (chris.hall@uit.no)

F. J. Mulligan, Department of Experimental Physics, National University of Ireland, Maynooth, Ireland.

M. Tsutsumi, National Institute of Polar Research, 9-10, Kaga 1-chome Itabashi Itabashi-ku, Tokyo 173-8515, Japan.